IDEA
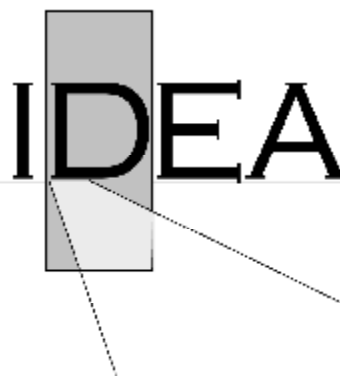
Innovations Deserving Exploratory Analysis Programs

Highway IDEA Program

SCANNING CAPACITIVE ARRAYS FOR REAL-TIME, IN-SITU IMAGING OF DENSITY AND THICKNESS IN HMA ROADWAYS

Final Report for Highway IDEA Project 138

Prepared by:
Yanko Sheiretov and Robert Lyons, JENTEK Sensors, Inc

September 2009

TRANSPORTATION RESEARCH BOARD
OF THE NATIONAL ACADEMIES

**INNOVATIONS DESERVING EXPLORATORY ANALYSIS (IDEA)
PROGRAMS
MANAGED BY THE TRANSPORTATION RESEARCH BOARD (TRB)**

This NCHRP-IDEA investigation was completed as part of the National Cooperative Highway Research Program (NCHRP). The NCHRP-IDEA program is one of the four IDEA programs managed by the Transportation Research Board (TRB) to foster innovations in highway and intermodal surface transportation systems. The other three IDEA program areas are Transit-IDEA, which focuses on products and results for transit practice, in support of the Transit Cooperative Research Program (TCRP), Safety-IDEA, which focuses on motor carrier safety practice, in support of the Federal Motor Carrier Safety Administration and Federal Railroad Administration, and High Speed Rail-IDEA (HSR), which focuses on products and results for high speed rail practice, in support of the Federal Railroad Administration. The four IDEA program areas are integrated to promote the development and testing of nontraditional and innovative concepts, methods, and technologies for surface transportation systems.

For information on the IDEA Program contact IDEA Program, Transportation Research Board, 500 5th Street, N.W., Washington, D.C. 20001 (phone: 202/334-1461, fax: 202/334-3471, http://www.nationalacademies.org/trb/idea)

SCANNING CAPACITIVE ARRAYS FOR REAL-TIME, IN-SITU IMAGING OF DENSITY AND THICKNESS IN HMA ROADWAYS

IDEA Program Final Report

Project NCHRP-138

Prepared for

The IDEA Program
Transportation Research Board
National Research Council

by

Yanko Sheiretov and Robert Lyons

JENTEK Sensors, Inc.
110-1 Clematis Ave
Waltham, MA 02453

Tel: (781) 642-9666
Fax: (781) 642-7525
E-mail: jentek@shore.net

September 2009

TABLE OF CONTENTS

LIST OF FIGURES

ACKNOWLEDGEMENTS

Patents issued and pending

EXECUTIVE SUMMARY

IDEA Concept and Product HMA density is one of the best predictors of highway durability. This project seeks to leverage JENTEK's novel capacitive sensor array technology, data acquisition instrumentation, inverse methods, and software to enable rapid, wide-area registered imaging of HMA density and thickness. The idea is to measure and analyze the frequency response of the JENTEK sensor at each of many individual locations, using electric fields penetrating to various depths inside and through the HMA, and thereby estimate the permittivity, conductivity, and thickness of the HMA. The observed correlation of permittivity with HMA density (Figure 3) should enable the desired density vs. location information.

Project Results/Planned Investigation In each of the two stages of this IDEA Phase I project, a set of specimens and a sensor were created and used to correlate permittivity with density. Although each stage's specimens and sensor were constructed quite differently, there was good agreement between the two permittivity-density correlations. Figure 1 depicts the more practical Stage 2 sensor and one of the corresponding Stage 2 specimens, along with a schematic of how a staggered array of such sensors could be used to scan a roadway. Figure 2 presents an overview of the Stage 2 sensor's electrode design. Figure 3 presents the Stage 2 results. In addition to demonstrating reproducible density measurement feasibility, the IDED[*] also showed reproducible local (apparent) property variations.

At the June 5, 2009 presentation at Woods Hole, MA there was some discussion of the origin of these apparent property variations. Since then, a closer inspection of these specimens revealed significant variations in the thickness of two of the slabs. It is likely that these thickness variations are one significant source of the observed (apparent) local property variations – the data processing algorithm used in this study had assumed constant slab thickness. Thus, in follow-on efforts, independent thickness and density measurements will be required and a larger set of samples with both thickness and density variations should be included (see the Discussion section for further detail).

Product Pay-Off Potential Acquiring accurate and rapid HMA density measurements during construction will extend a highway's useful life, thereby minimizing the cost per year for the original construction. This technology may also prove useful for measuring soil density before construction, and for monitoring roadway degradation in-service.

Product Transfer We plan to apply for Highways for LIFE Technology Partnership funding (and pursue other funding opportunities) to further develop and test this technology – to incorporate independent density (permittivity), conductivity, and thickness imaging, to investigate the permittivity vs. density correlation for various HMA mixes and moisture levels, to evaluate options for cabling between the individual sensors in our capacitive sensor (IDED-Array), and to understand the significance of the apparent local property variations mentioned above.

[*]IDED: Interdigitated Electrode Dielectrometer
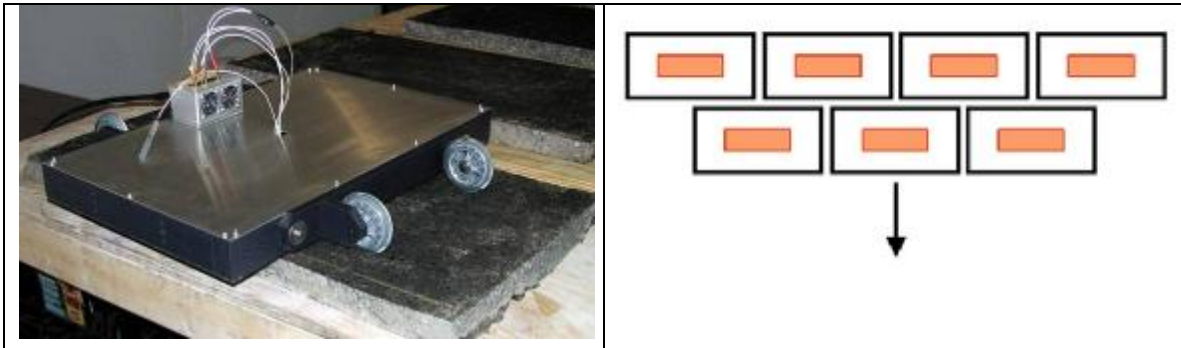
Figure 1, left: prototype rolling capacitive HMA density sensor scanning an HMA slab. Figure 1, right: schematic of seven such sensors in a staggered array designed to be rolled down a roadway to generate a rapid image. The orange center of each box represents the sensor's active region; staggering in this manner allows full coverage.
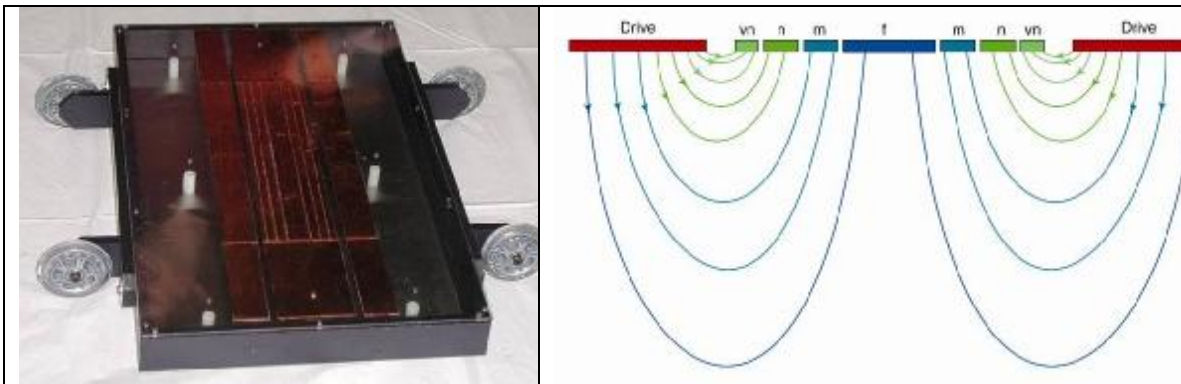
Figure 2, left: underside of the sensor in Figure 1. Note the capacitive sensing elements which generate and sense fields penetrating various depths into the HMA (see Figure 2, right). This patented approach enables HMA permittivity measurements that correlate with density (see Figure 3, below), independent of sensor lift-off (proximity).
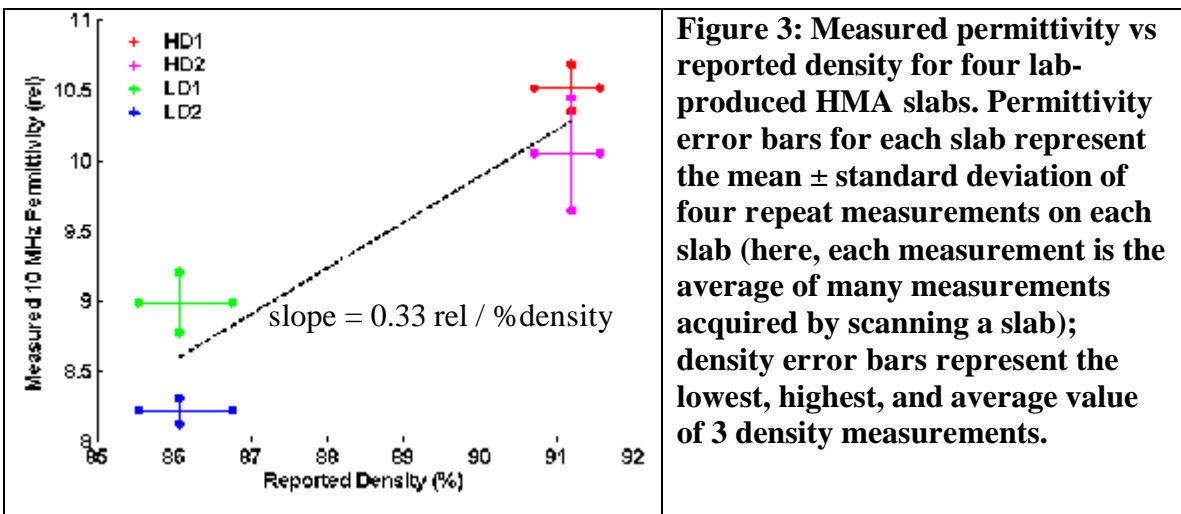
Figure 3: Measured permittivity vs reported density for four lab-produced HMA slabs. Permittivity error bars for each slab represent the mean ± standard deviation of four repeat measurements on each slab (here, each measurement is the average of many measurements acquired by scanning a slab); density error bars represent the lowest, highest, and average value of 3 density measurements.

Patents issued and pending

STAGE 1 WORK

Figure 4 depicts the nine Superpave 12.5 mm specimens analyzed in Stage 1. Each specimen had been cut in half to allow access to the center of the simulated core, so that 18 half-cores appear in the photo. Table 1 summarizes the density ranges spanned by these specimens.

Figure 5 depicts the DS05 sensor used to interrogate the Stage 1 specimens. Figure 6 shows a schematic of the DS05, with electrode segments and electric field lines color coded to illustrate the relative depths of sensitivity for the near, mid, and far sensing electrodes.

Figure 7 depicts the equipment set-up used to acquire the Stage 1 data. Note the half-core specimen covered in protective insulating film, the DS05 sensor, probe electronics, JENTEK admittance (or impedance) measurement instrumentation, and a computer running JENTEK's GridStation data acquisition and analysis software environment.

Figure 8 presents 3-unknown data acquired on these Stage 1 specimens. The three unknowns (conductivity, permittivity, and sensor lift-off) were calculated from 6.31 MHz data, with one complex admittance data point measured for each one of the three sensing electrodes. JENTEK's proprietary data multivariate inverse method was then used to search a pre-computed database of DS05 sensor responses and determine the properties most likely to have yielded the measured admittances.

The most important feature of this data is the monotonic ~0.12 rel / %density increase of permittivity with measured density (an Archimedes-type density measurement, performed by Prof. Walaa Mogawer of University of Massachusetts Dartmouth) for both the blue and black lines over the entire 86% to 97.1% density range.

Figure 9 depicts the experimental arrangement used to acquire the data presented in Figure 8. Figure 8's blue data was acquired using the physical registration map depicted in Figure 10. For each of six distinct measurement sessions, property data acquired at nine locations on each of three particular half-core specimens was averaged and presented as a single 'simulated large sensor' measurement. The black data was acquired by taking 6 unregistered measurements on each of the six half-core specimens in each density range.

The fact that the six simulated large sensor measurements on each specimen agree well with each other relative to the full ~1.3 rel permittivity excursion across the density range (blue data; note especially the small standard deviations for medium and high densities), and also agree reasonably well with the black 'average over all specimens in each density range' data, suggest that a large sensor could plausibly average over the 'material noise' associated with the HMA's course granularity and yield a robust permittivity well correlated with density. This is borne out in the Stage 2 analysis.

Patents issued and pending
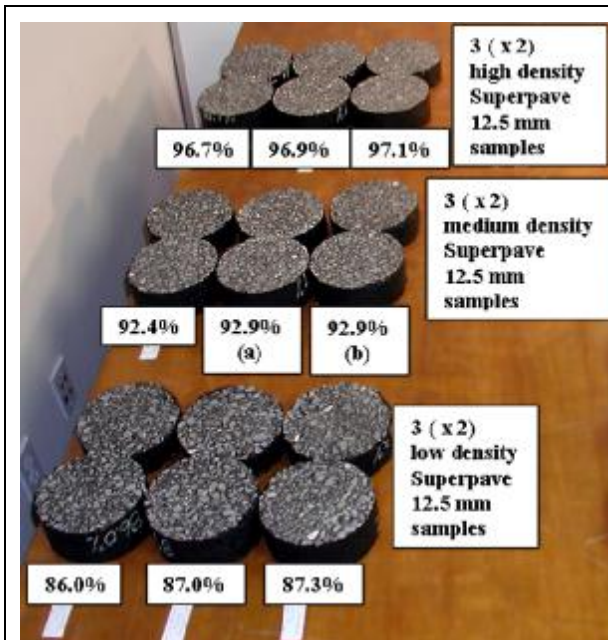
Figure 4:

Reported densities, and density ranges, of 9 Superpave 12.5 mm samples.

	Density (%)	Density Range (%)
High	96.7, 96.9, 97.1	96.9 ± 0.2
Medium	92.4, 92.9, 92.9	92.65 ± 0.25
Low	86.0, 87.0, 87.3	86.65 ± 0.65

Table 1: Reported densities, and density ranges, of 9 Superpave 12.5 mm samples.
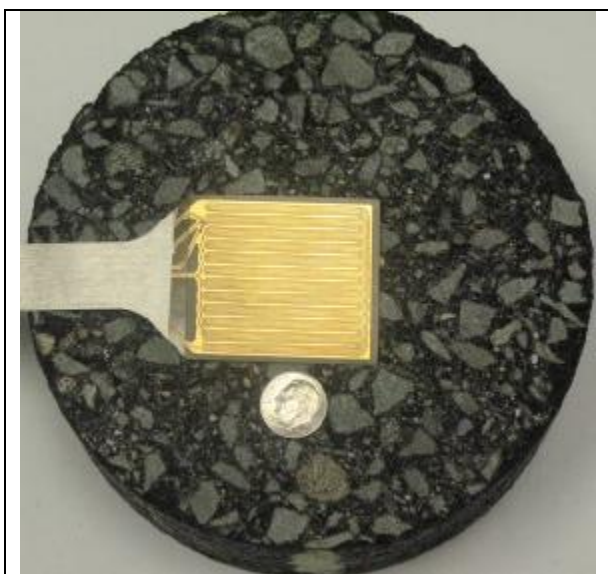
Figure 5: A DS05 sensor atop a low density (86%) Superpave 12.5 mm sample. The electrodes are facing away from the sample in this photo, so their scale can be compared with the stones in the HMA; during measurement the electrodes face the sample. A dime is included in the photograph for scale.

Patents issued and pending
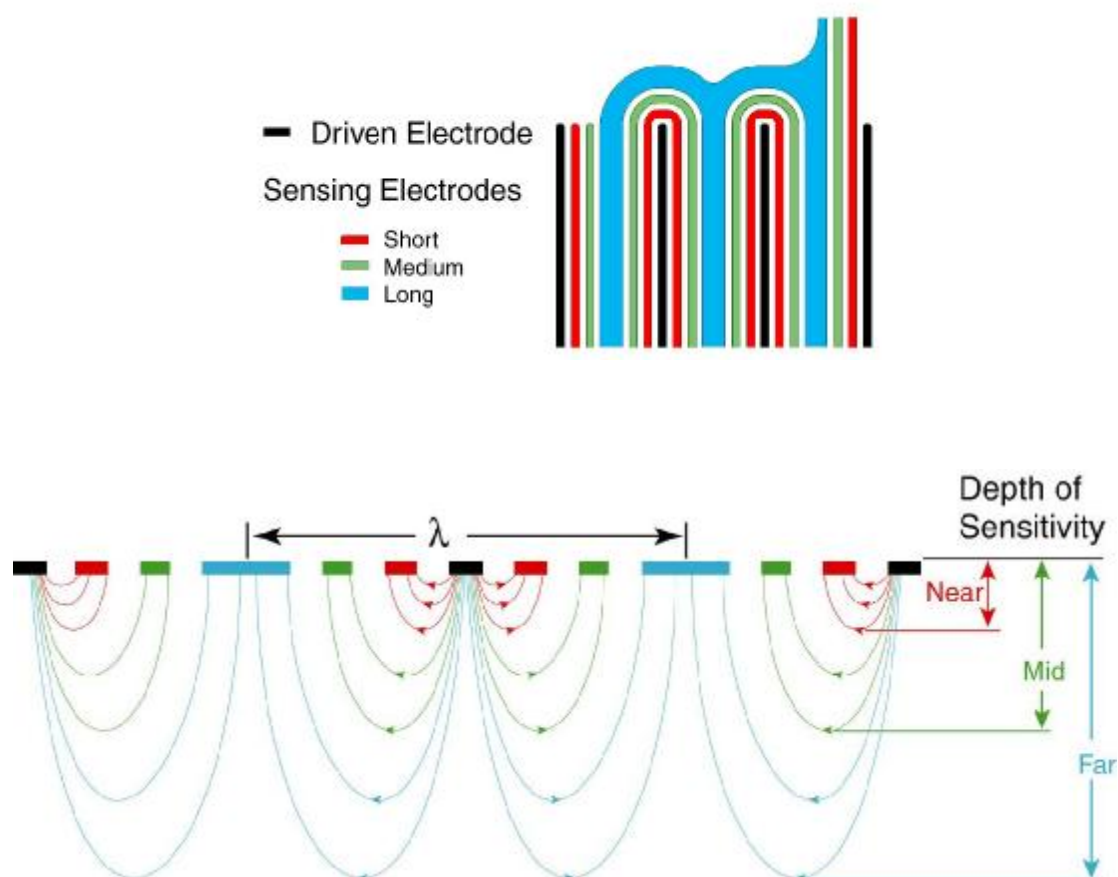
Figure 6: Schematic of the segmented-field electrodes. Each sensing element responds to a different component of the electric field.

Patents issued and pending
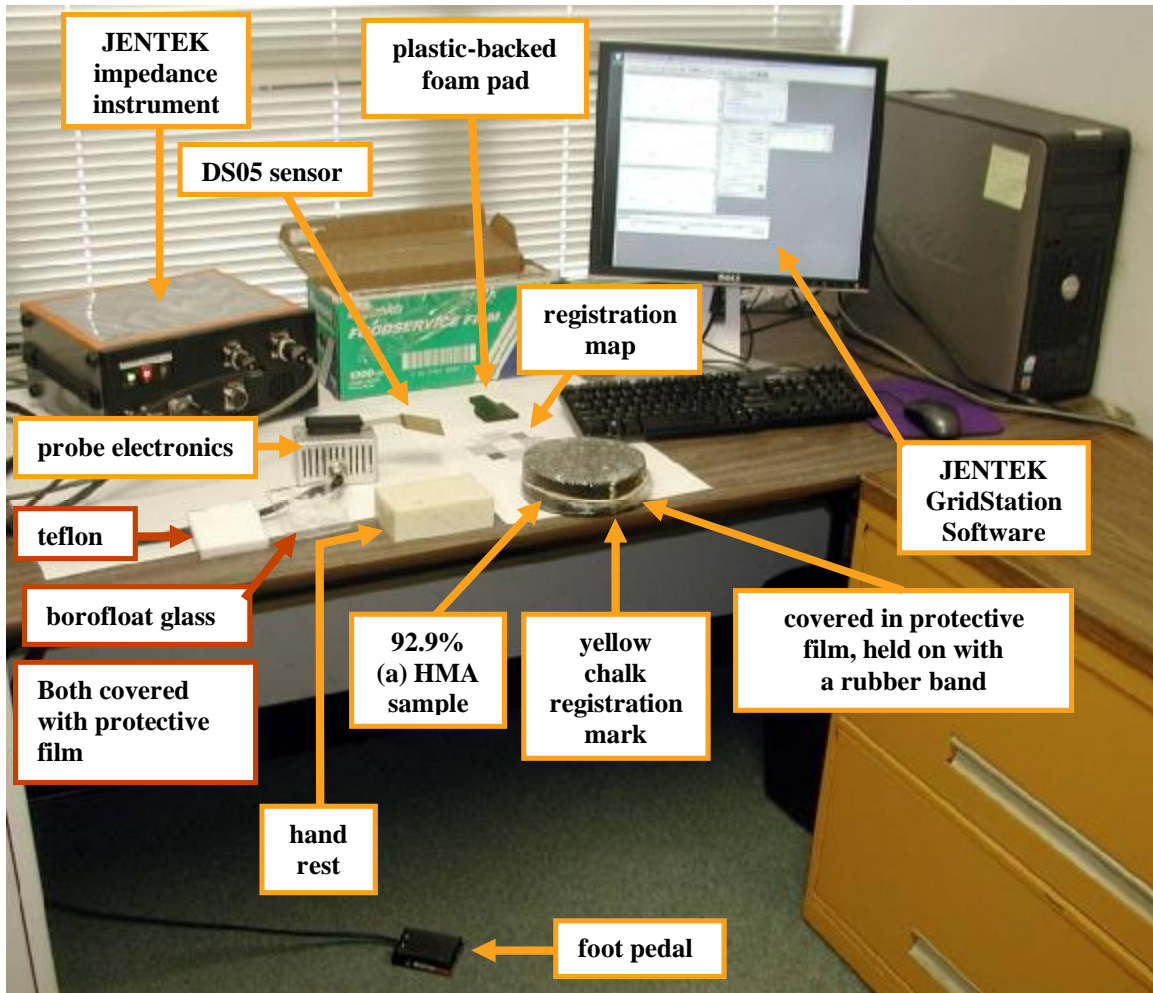
Figure 7: Stage 1 HMA sample, the DS05 sensor, probe electronics, JENTEK impedance measurement instrumentation, and a computer running JENTEK's GridStation data acquisition and analysis software environment. Note Teflon and borofloat glass specimens used for calibration, and plastic-backed foam pad for delivering even pressure over the sensor during measurement.

Comparison of DS05 measurements on the entire population with simulated large IDED measurements on 3 representative samples

6.31 MHz
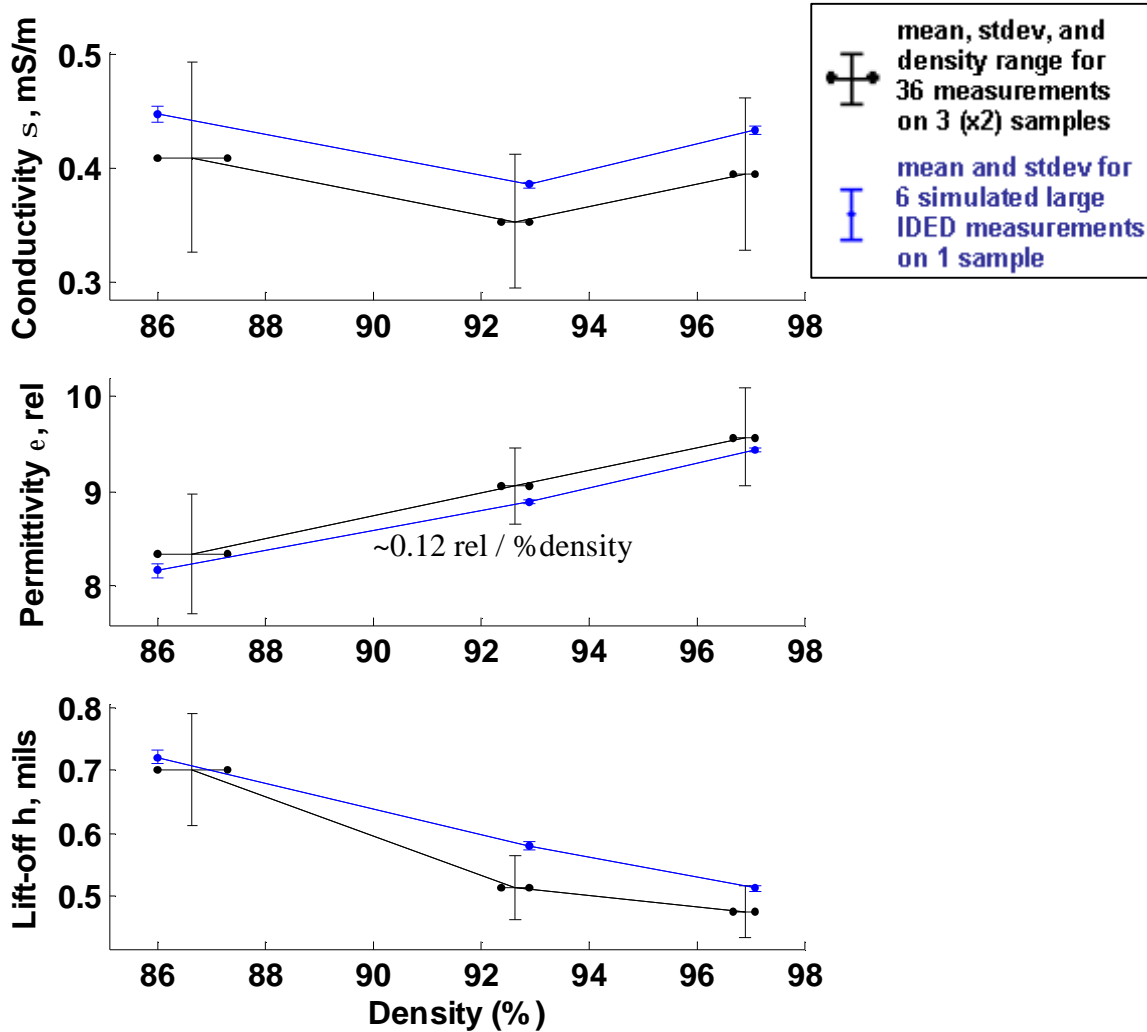
Figure 8: Comparison of the mean and scatter of the 6.31 MHz data vs reported density. Black data: 36 physically un-registered measurements on 3 (x2) samples in each density range. Blue data: 6 pick-and-place measurements of a simulated large IDED sensor (each plotted symbol represents the mean of the property values at 9 physically registered locations).

Figure 9: Measurement at location 1 on sample 9.29% (a) .
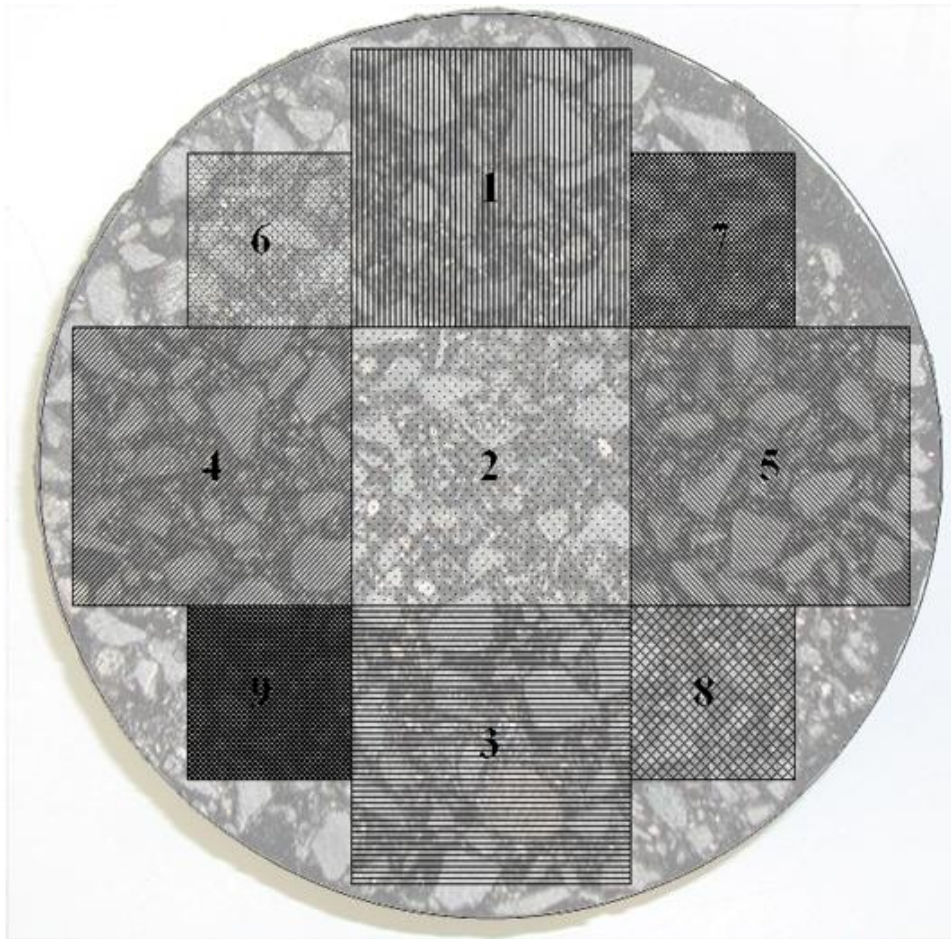
Figure 10: HMA sample with measurement location registration map superimposed.

STAGE 2 WORK

Figure 11 presents the four slab-shaped Stage 2 specimens. The two low density specimens, LD1 & LD2, have reported density (86.1± 0.6)%. The two "high" density specimens, HD1 & HD2, have reported density (91.2 ± 0.4)%. Note that, on the low, middle, and high density scale of the Stage 1 specimens, these Stage 2 specimens only span from low to middle density. The specimens were reported to be approximately 1.5 inches thick, with approximately 1/8 inch variability.

Figure 12 offers a schematic presentation of the method used to create the Stage 2 specimens. Note that the specimens were created in pairs, with 6 compressor passes used to create specimens LD1 and LD2, and 20 compressor passes used to create HD1 and HD2. The initial volume of raw HMA used the create the specimen-pairs was not carefully controlled, nor was the area over which this volume was initially spread, so it does not follow that the HD specimens are thinner than the LD specimens.

After the specimen pairs were extracted, the material surrounding the specimens was collected and analyzed via Archimedes' method to estimate the density of the specimens themselves.

Figure 13 shows the Stage 2 sensor scanning one of the Stage 2 specimens; the underside of the sensor; and, the four major component parts comprising the sensor.

Figure 14 exhibits a set of conceptual stages transitioning from a parallel plate capacitor (a simple dielectrometer) to a segmented field dielectrometer. Both the Stage 1 and Stage 2 sensors are segmented field dielectrometers. The four electrodes in the final, fourth stage (bottom right) are labeled 'f' for far, 'm' for middle, 'n' for near, and 'vn' for very near.

Figure 15 presents the generic dielectrometer model used to design the Stage 2 sensor. It was used to ensure measurable signal levels and sensitivity to desired HMA properties (*e.g.*: permittivity, conductivity, thickness) by assuming a likely lift-off and investigating the sensor's modeled response given various sensor geometry parameters (*e. g.*: the size of the backplane gap, the widths of various electrodes and the gaps between them). This model also applies to the DS05 dielectrometer used in the Stage 1 analysis.

Figure 16 presents two measurement grids for the far electrode of the Stage 2 sensor, one for 10.0 kHz and one for 6.31 MHz.

Figure 17 presents electrode widths and approximate electric fields for the Stage 2 sensor. Note that the two halves of the drive electrode (colored red, located farthest from the center point of the sensor) are connected electrically so that they comprise a single electrode. Similarly: the far, mid, and near sensing electrodes appear physically split but are actually a single piece of metal, and are measured as such. The far sensing electrode appears in the center of the diagram.

Figure 18 presents a schematic of electrode width and lengths as placed in the actual sensor. Note that all active electrodes are 12 inches long, but some of the 'dummy' guard electrodes are also visible in this schematic.

Figure 19: Schematic of all the electrodes as they actually sit in the sensor. Compare with the upper right photo in Figure 13.

Figure 20 depicts a measurement grid representing the pre-computed admittance responses used to analyze the Stage 2 data. This is called a 10 MHz Mid/Far Mag-Mag Permittivity/Lift-off Grid assuming zero conductivity and specimen thickness = 1.5 in.

Note that for this exploratory analysis only the magnitude of the middle and far sensor responses at 10 MHz was used, and that only the material permittivity and sensor lift-off were considered as unknowns to be determined; the material conductivity and specimen thickness were assumed known and fixed. This simplifying assumption was necessary given budget and time constraints, but is not an inherent limitation to this sensing technology.

Figure 21 depicts the results of two separate permittivity scans of specimen LD1. To compute these scans, at each individual location the magnitude of the complex 10 MHz admittance was computed for the middle and far channels and JENTEK's proprietary multivariate inverse method software was used to compute the {permittivity, lift-off} property pair most consistent with the measured data. Only the permittivity results are shown in these plots.

Each scan started with the 'near' pair of sensor wheels close to the near end of the specimen, then traversed down and back, and down and back again. The point of the repeat scans was to look for any repeatable features in the data as a function of position, and not confuse material noise (variation associated with the sample) with measurement noise (variation associated with the sensing apparatus).

These scans were acquired in approximately 9 seconds and are comprised of approximately 900 points, so one 10 MHz data point was acquired every 0.01 seconds. However, during the same 9 second duration, data at 631 kHz and 6.31 MHz was acquired as well.

It turned out those frequencies need not have been acquired, because the 10 MHz data alone was sufficient for proof of concept. Future iterations of this application may use the multiple frequency data. Especially, if an additional unknown thickness layer of upper surface moisture corresponding to rain-soaked asphalt needs to be accounted for. The point is that this data *could have been* acquired while moving the sensor at three times the speed with no loss of spatial resolution because, if only the 10 MHz data had been acquired, the data rate would have been 300 samples per second instead of 100 samples per second.

Patents issued and pending

Note the repeatable features in Figure 21, with a series of {low, high, low, high} permittivities being registered as the sensor travels down the sample, and again (backwards) as the sensor comes back. This pattern is repeated twice in each scan, with this entire pattern repeated in both scans. This pattern must therefore be associated with some property of this specimen, and cannot be an artifact of sensor noise. Possible specimen properties that may cause this behavior are discussed in the next section.

For now, note in Figure 22 how each specimen has its own signature. Four such scans were acquired on each specimen.

In Figure 23, the four permittivity scans on each specimen were reduced to four permittivities by averaging all ~900 measurements in each scan to a single permittivity. The resulting mean and standard deviation for each specimen are plotted along with the lowest, highest, and mean of three reported density measurements for each specimen (recall that the specimens were created in pairs, so both the lower density specimens have the same reported densities; and similarly, for the two higher density specimens). There is a clear separation between the permittivities associated with the lower and the higher density specimens, and the average slope is 0.33 rel / %density.

Note that these Stage 2 slab specimens only represent a 5.1% density range (from 86.1 to 91.2 %density), whereas the Stage 1 specimens represent a 10.2% density range (from 86.7 to 96.9 %density). Our understanding is that the wider Stage 1 density range is more representative of HMA densities occurring in the field, so the full range of permittivities observed in the field are likely to be approximately twice the range appearing in Figure 23.
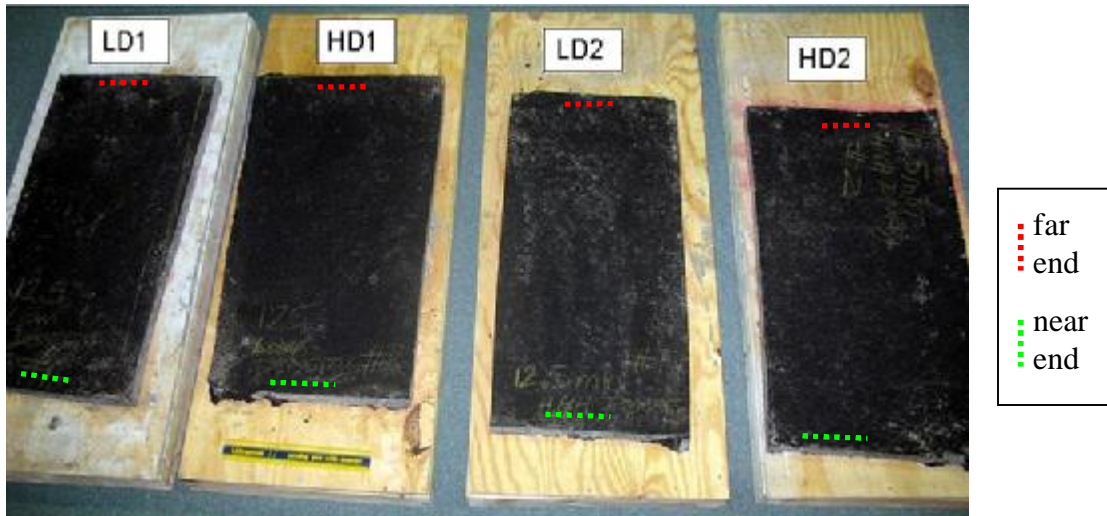
Figure 11: Four slab specimens of typical 12.5 mm SuperPave. On the low, middle, and high density scale of the Stage 1 specimens, specimens LD1 and LD2 (86.1± 0.6 % dense) correspond to low density but specimens HD1 and HD2 (91.2 ± 0.4 % dense) correspond to middle density, not high density.
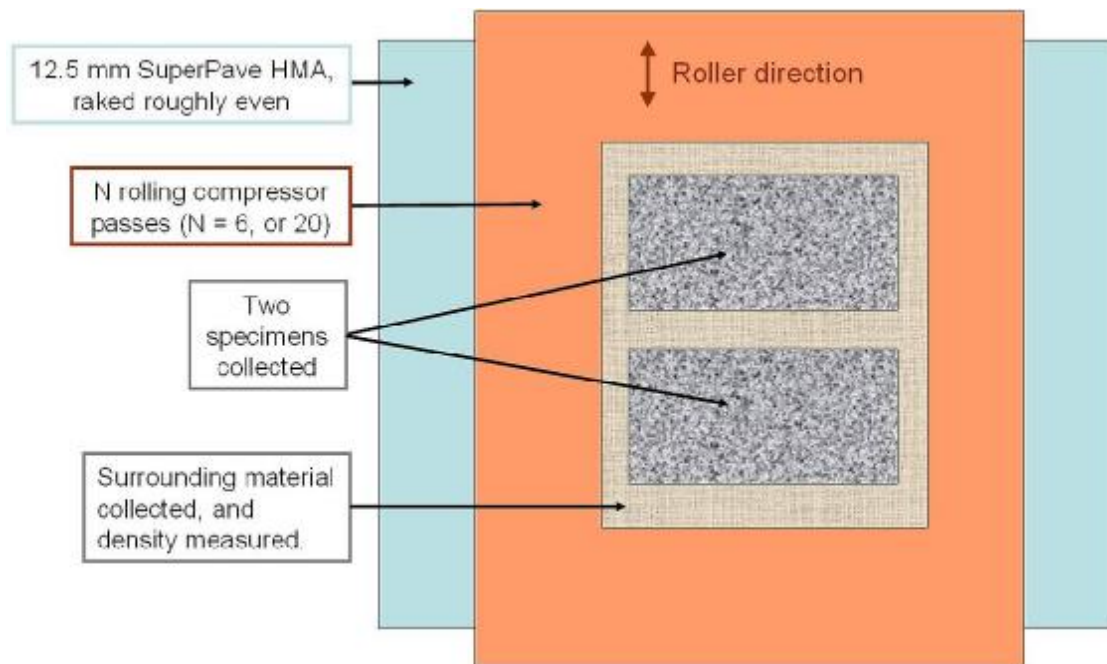
Figure 12: Schematic presentation of the method used to create the four Stage 2 specimens. The two lower-density slab specimens (LD1 & LD2) were created together using 6 rolling compressor passes; the two higher-density slab specimens (HD1 & HD2) were created using 20 rolling compressor passes.

Patents issued and pending
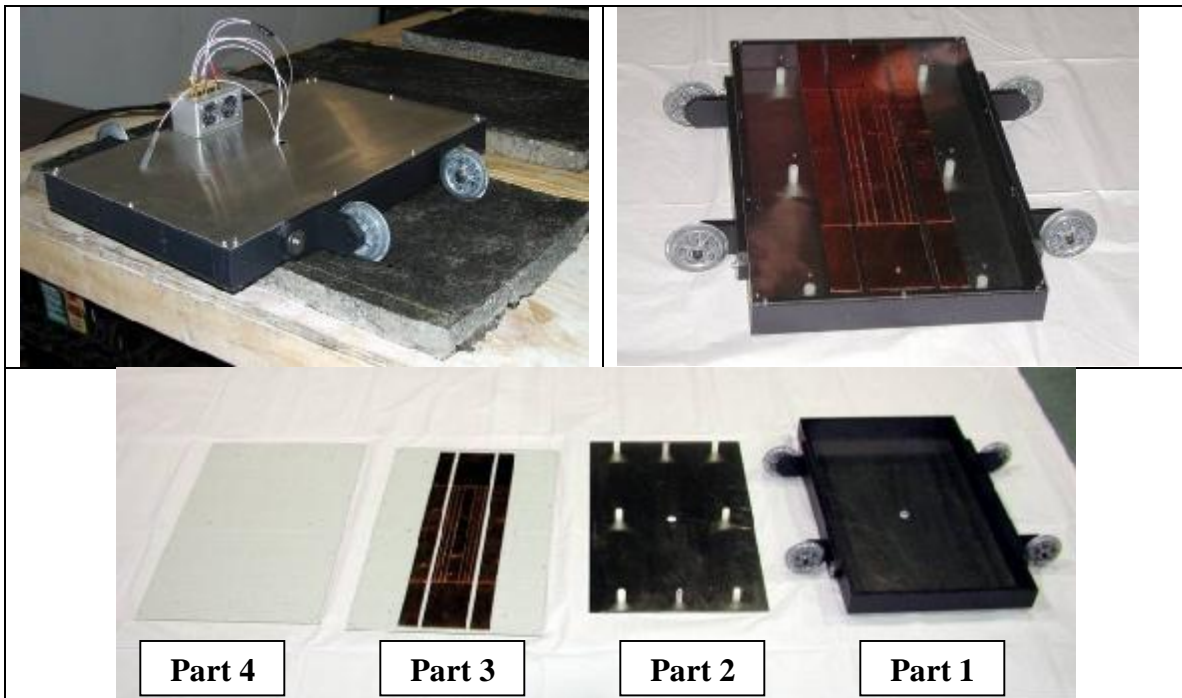
Figure 13) Upper left: Stage 2 sensor atop a slab HMA sample. Upper right: bottom view of the sensor. Bottom row: the four major component parts of the sensor.
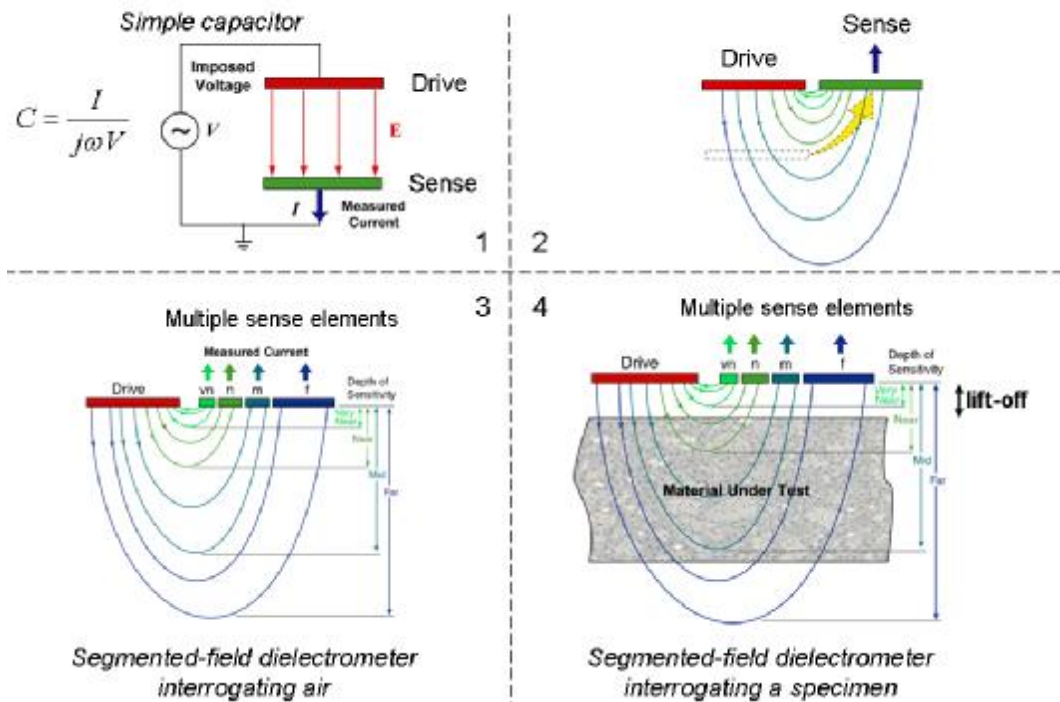
Figure 14: Conceptual stages transitioning from a simple dielectrometer (a parallel plate capacitor) to a segmented field dielectrometer.

Patents issued and pending
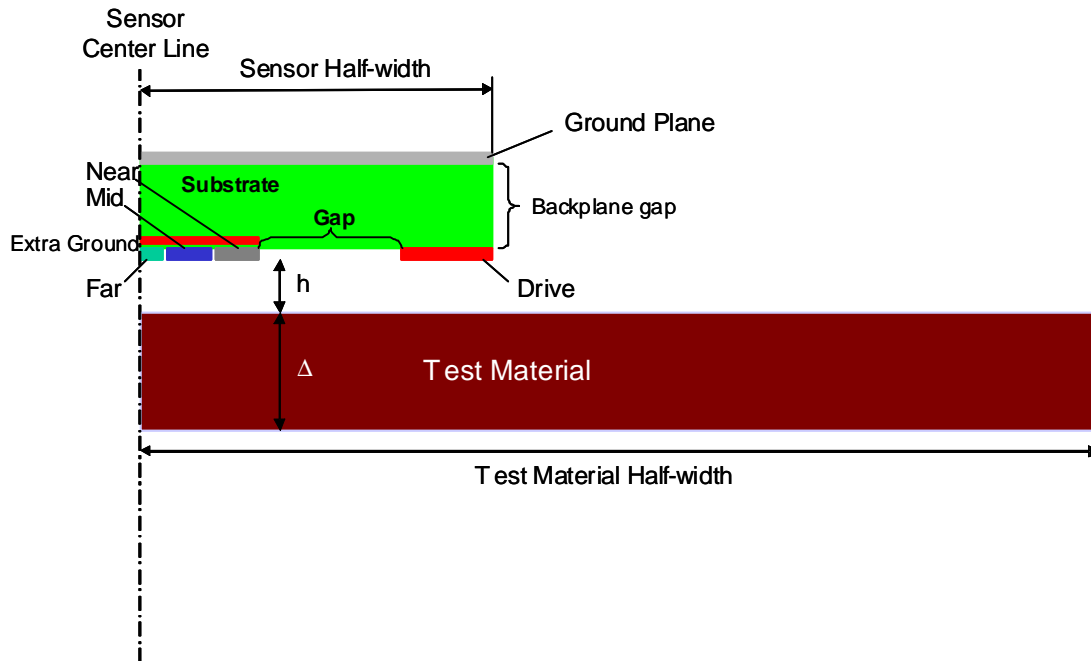
Figure 15. Cross-sectional view of dielectrometer simulation geometry.
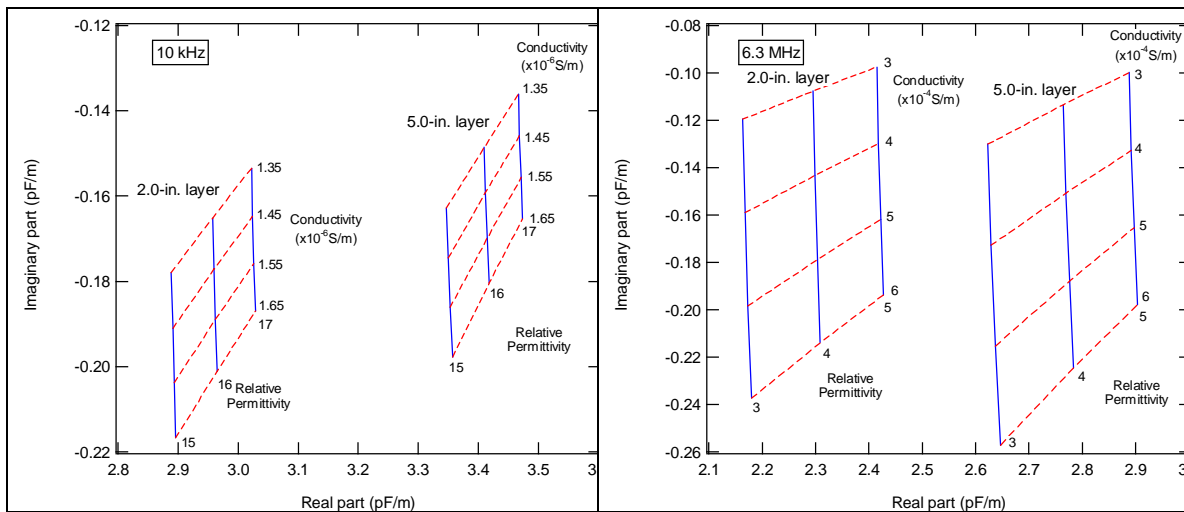
16. Measurement grids for the far channel sense element at 10.0 kHz and 6.31 MHz.
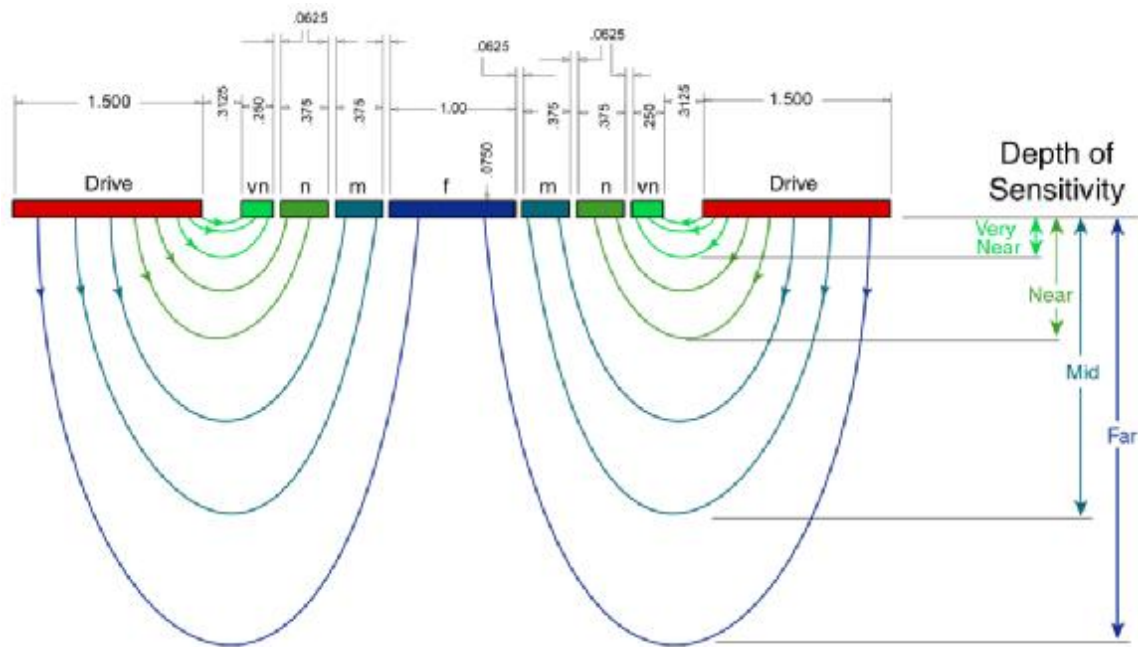
Figure 17: Electrode widths and approximate electric fields for the Stage 2 sensor.
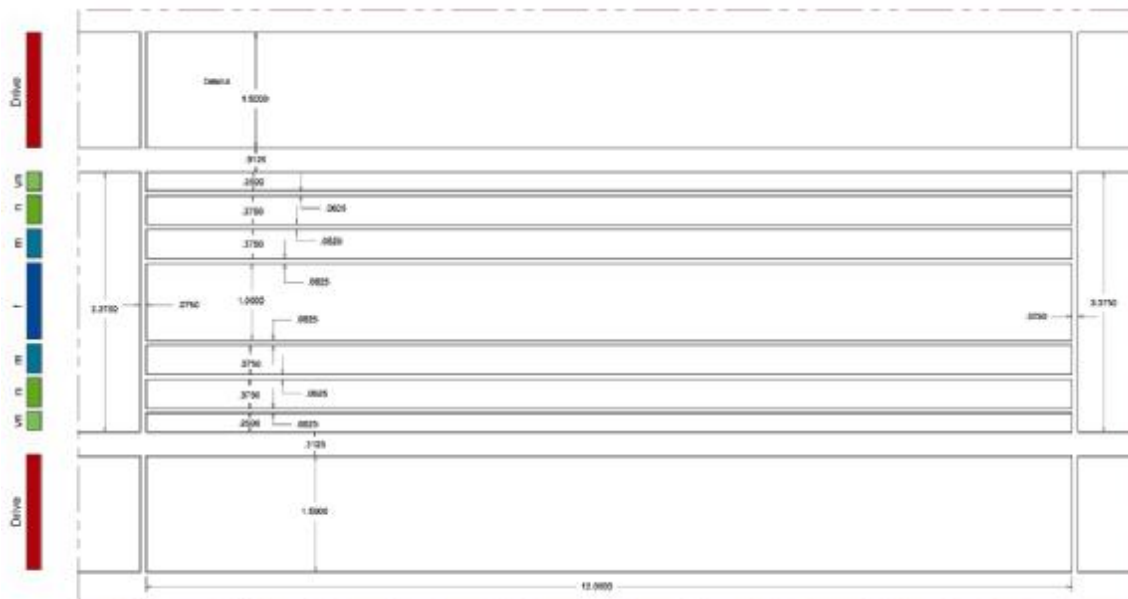
Figure 18: Schematic of electrode width and lengths as placed in the actual sensor.
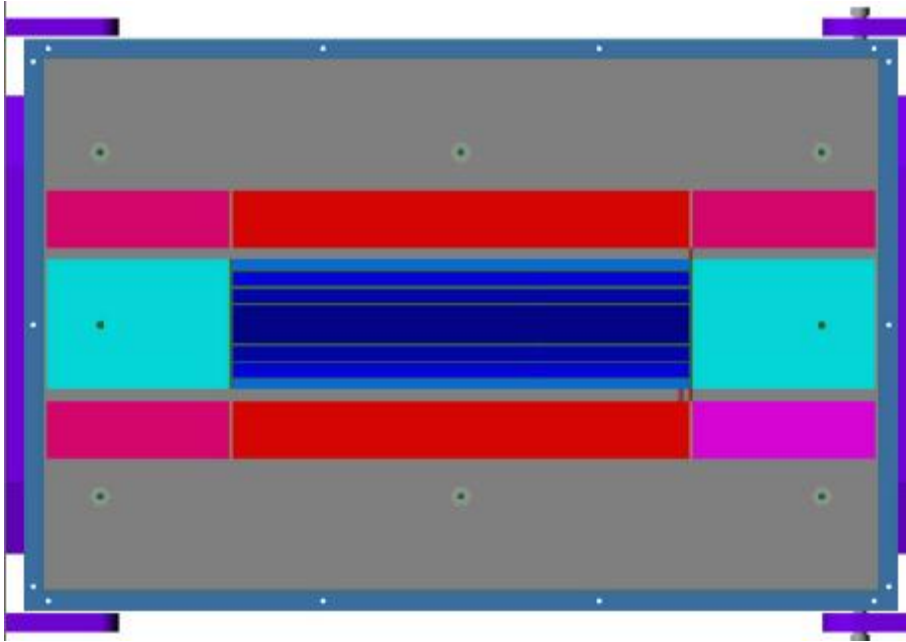
Figure 19: Drive, sense, and guard electrodes, as placed in the sensor cart.
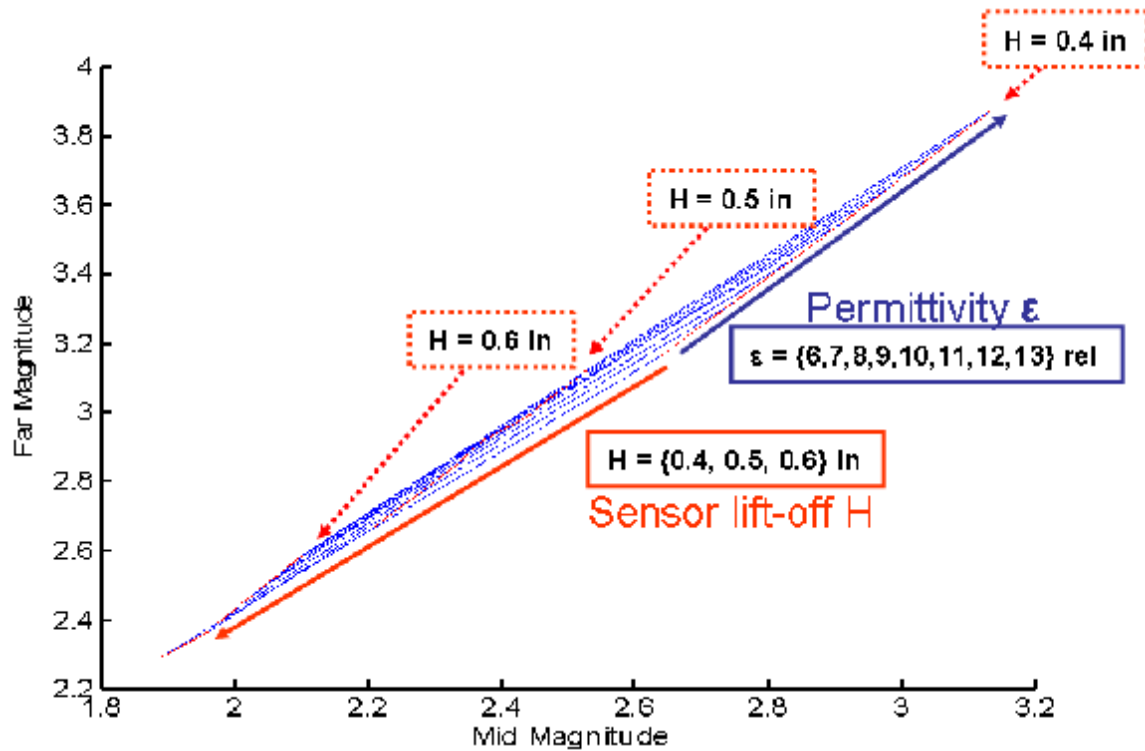
Figure 20: Measurement grid representing the pre-computed admittance responses used to analyze the Stage 2 data. This is a 10 MHz Mid/Far Mag-Mag Permittivity/Lift-off Grid assuming zero conductivity and specimen thickness = 1.5 in. Dotted lines and boxes show the location of the three distinct "lift-off = constant" lines corresponding to a 6 to 13 rel range of permittivities.
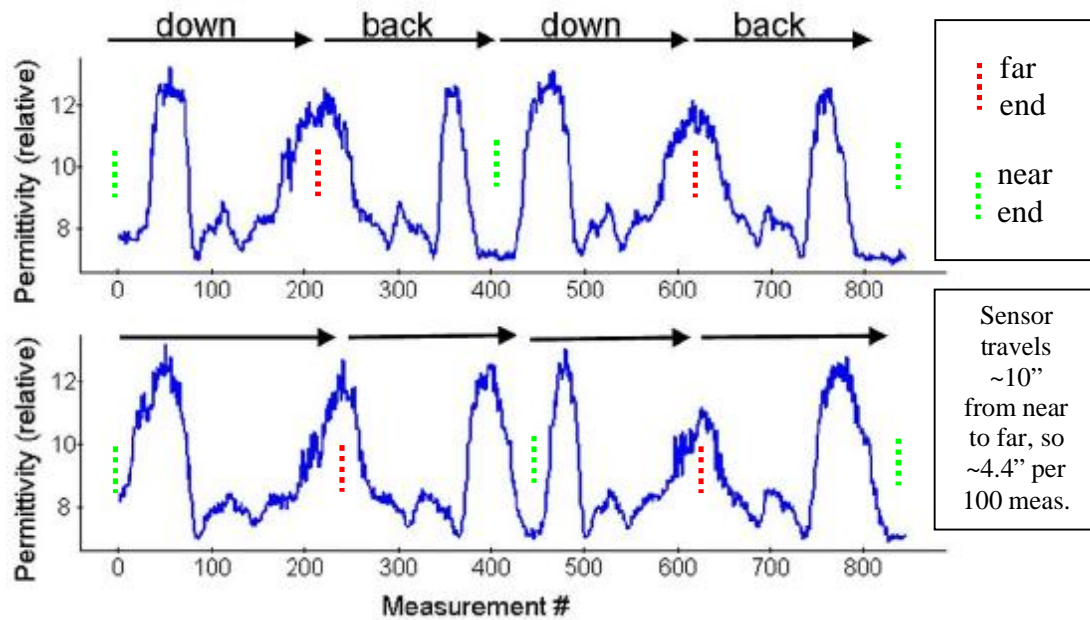
Figure 21: 2 repeat scans of specimen LD1 (of 4 total acquired on this specimen)
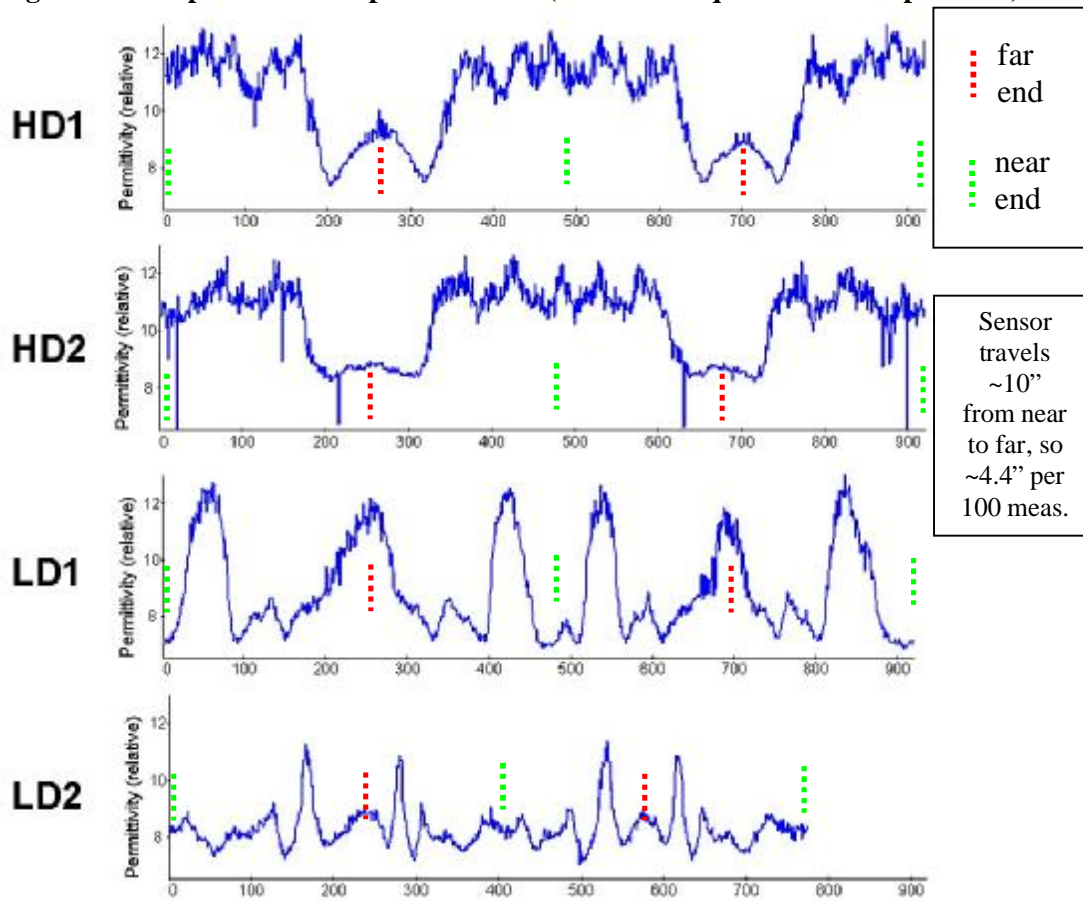
Figure 22: one representative scan on each specimen.

Patents issued and pending
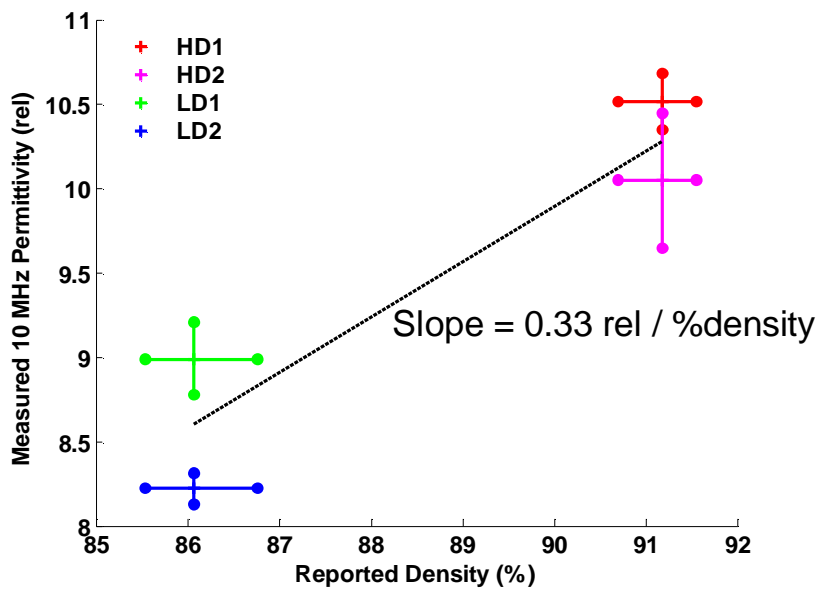
Figure 23: Mean ± standard deviation of 4 repeat permittivity measurements on each of the 4 specimens. 3 density measurements were reported for the low density specimens, and similarly for the high density specimens. Plotted x-values depict the lowest, highest, and mean values for each density.

DISCUSSION

Reproducible local (apparent) property variations

We discovered that both HD specimens exhibited up to 0.5 inches of thinning or loss (an approximately 33% reduction from the nominal thickness of 1.5 inches) over a 6 inch region at the far end of the specimens. Figure 24 shows this loss region on specimen HD2. Figure 25 shows a detail from Figure 22 showing only the permittivity of the HD specimens, with measurement numbers corresponding to these loss regions emphasized. The permittivity definitively drops in these regions.

The other observed (apparent) local property variations may be the result of this type of thickness variation, or a density variation, or a conductivity variation, or all of the above. A more detailed analysis of a larger, more well-controlled set of specimens and/or samples is required to resolve this issue.

For now the following two observations are offered to help eliminate concern that the LD specimens may simply be, on average, thinner than the HD specimens -- so that the observed average permittivity difference is actually due to a thickness difference, rather than a density difference. First: the Stage 1 analysis registered a definite positive correlation of permittivity with density despite the specimens being effectively infinitely thick (relative to the penetration depth of the DS05 sensor). Second: thickness measurements on specimens LD2 and HD2 found them to be of nearly identical thickness in their middle-to-near region, yet the permittivity difference between these specimens in this region is quite clear.

Apparent efficacy of the measurement approach

Having addressed the origin of the anomalously low permittivity measurements occurring near the far side of the HD specimens, if the data in Figure 23 were re-plotted without the anomalous data the average HD measurement would move from ~ 10.2 rel to at least 11 rel, maybe 11.5 rel, resulting in an even stronger discernment of density. Bear in mind that the Stage 2's LD and HD specimens only span from low- to middle-density in terms of the Stage 1 specimens' more broad and practical density range. We should expect the Stage 2 sensor to measure permittivies ~ 13.5 to 14 for high density samples. Further: note that Figure 8's blue permittivity data shows a measurement standard deviation that decreases with density, so we can hope for less noise (and therefore better density discernment) at the higher densities likely to be associated with finished HMA.

Although neither the Stage 1 nor the Stage 2 analyses allowed for thickness as an independently-measured unknown, the sensor's response to the thinning evident at the far ends of the HD specimens suggests that the middle and far electrodes of the Stage 2 sensor have plenty of thickness sensitivity. We could pursue thickness as an independent unknown in follow-on work (we have had success with this type of approach using our more-advanced line of inductive sensors),*or* we could simply use the sensors 'very near'

20

and 'near' elements to try to measure only the density of the HMA near the surface (that is, remove the thickness sensitivity).

Conclusions / Plans for implementation

We believe these results show our product to be a viable candidate for rapid HMA density measurement. In Figure 1, right, we show a schematic diagram of how seven of these sensors could be arranged to allow full coverage of a four-foot scan path. The admittance-measurement instrument used to acquire the data analyzed in this report is capable of acquiring multi-frequency data on up to 38 channels simultaneously. So the relatively simplistic mid/far electrode approach used in this report could be applied to 19 sensors, optionally allowing for full coverage of a 10 foot wide scan path with a single instrument. JENTEK already has the software required to analyze and image this type of data in near real time.

We plan to apply for Highways for LIFE Technology Partnership funding (and pursue other funding) to further develop and test this technology – to allow for independent density (permittivity), conductivity, and thickness measurement and imaging, to investigate the permittivity vs. density correlation for various HMA mixes and moisture levels, to evaluate options for cabling between the individual sensors in an IDED-Array, and to understand the significance of the apparent local density variations observed on these specimens.

Patents issued and pending

Figure 24: Loss region, viewed from the right side of the far end of specimen HD2.
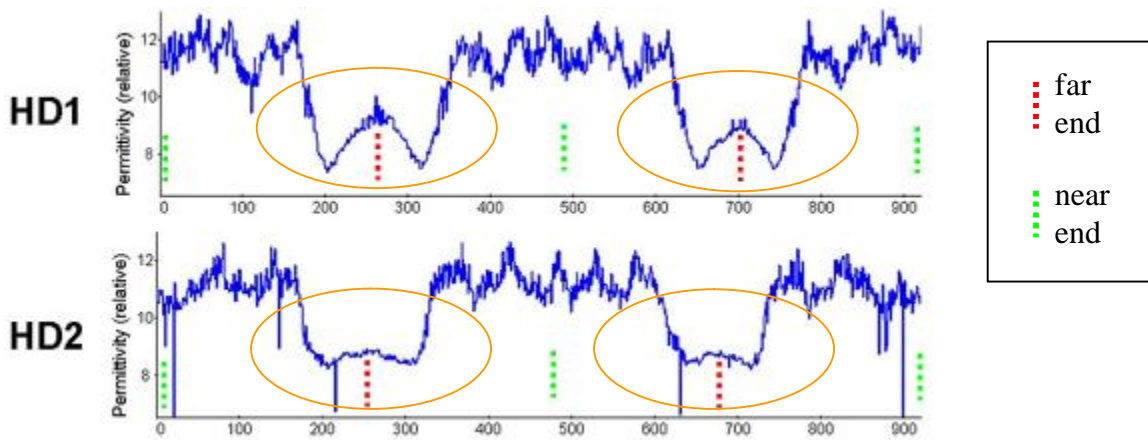

Figure 25: Permittivity measurements on the HD specimens, with orange ovals emphasizing data corresponding to regions of thinning or loss. Sensor travels ~10" from near to far, so ~4.4" per 100 meas.

APPENDIX A: DIELECTROMETRY PATENTS

1. Sheiretov, Yanko K.; Goldfine, Neil J.; Washabaugh, Andrew P.; Schlicker, Darrell E.; **"Material Property Estimation Using Non-Orthogonal Responsive Databases," U.S. Patent Number 7,467,057 B2**, December 16, 2008.

2. Goldfine, Neil.; Schlicker, Darrell E.; Zilberstein, Vladimir A.; Washabaugh, Andrew P.; Weiss, Volker; Craven Christopher A.; Shay, Ian C.; Grundy, David G.; Walrath, Karen E.; Lyons, Robert J.; **"Material Condition Monitoring with Multiple Sensing Modes," U.S. Patent Number 7,451,657 B2,"** November 18, 2008.

3. Goldfine, Neil J.; Schlicker, Darrell E.; Sheiretov, Yanko K.; Washabaugh, Andrew P.; Grundy, David C.; Zilberstein, Vladimir A.; **"*Segmented Field Dielectric Sensor Array for Material Characterization*," US Patent Number 7,280,940 B2**, October 9, 2007.

4. Goldfine, Neil J.; Schlicker, Darrell E.; Zahn, Markus.; Ryan, Wayne D.; Shay, Ian C.; Washabaugh, Andrew P.; **"*Inspection Method Using Penetrant and Dielectrometer*," U.S. Patent Number 6,781,387 B2**, August 24, 2004.

5. Goldfine, Neil J.; Schlicker, Darrell E.; Zahn, Markus; Ryan, Wayne D.; Sheiretov, Yanko K.; Washabaugh, Andrew P.; **"*Segmented Field Dielectrometer*," U.S. Patent Number 6,486,673 B1**, November 26, 2002.

6. Goldfine, Neil J.; Schlicker, Darrell E.; Washabaugh, Andrew P.; **"*Absolute Property Measurement with Air Calibration*," US Patent Number RE39,206 E**, July 25, 2006.

Patents issued and pending

APPENDIX B: KEY PERSONNEL

Principal investigators:

Dr. Yanko Sheiretov, Vice President, Product Development & Commercialization.

Dr. Sheiretov, Vice President, Product Development & Commercialization at JENTEK Sensors, is also the lead software architect responsible for the functionality of all software products. Additionally, he is also a major contributor to sensor and algorithm development. Dr. Sheiretov completed his Ph.D. degree in Electrical Engineering at the Massachusetts Institute of Technology. His doctoral thesis, entitled "Deep Penetration Magnetoquasistatic Sensors," describes research he conducted on integration of a GMR sensor with JENTEK's shaped field magnetic sensors. Dr. Sheiretov also has experience in several areas of Electrical and Computer Engineering and Applied Physics, including electromagnetic field and sensor analysis and modeling; solid state physics; power electronics; wireless telecommunications; analog and digital system design. His software development experience has focused on numerical methods, data modeling and analysis, and numerical estimation on a variety of platforms. He also has experience in GUI software design. Dr. Sheiretov holds B.S., M.S., E.E., and Ph.D. degrees from the Massachusetts Institute of Technology. He is a recipient of the 1992 Henry Ford II Scholar Award for Academic Excellence. Since joining JENTEK, Dr. Sheiretov has contributed to numerous patents and journal publications.

Dr. Robert J. Lyons, Senior Electrical Engineer, Senior Software Engineer.

Dr. Lyons has a Ph.D. in Electrical Engineering from M.I.T, and a Master of Science (MS) in EE from Boston University. He is a specialist in algorithm research; especially, signal processing for inverse problems. His computer language experience includes Matlab, Mathematica, LabVIEW, and C. Additionally, he has experience with inverse medium and inverse source problems in acoustics, atmospheric radiation, and electromagnetic settings. He also has experience in data compression of biomedical signals, speech, and images; and GUI design.

Other key contributors:

Dr. Andrew Washabaugh, Senior Vice President, Product Research & Development.

Dr. Washabaugh is a specialist in the development of sensors, instrumentation, and models for the electromagnetic, electromechanical, and electrochemical characterization of materials. Dr. Washabaugh has a Master's Degree, Engineer's Degree, and Sc.D. in Electrical Engineering from M.I.T., and a Bachelor's Degree in Electrical Engineering from the University of Michigan. He is a member and currently Membership Secretary for ASTM Committee E07 on Nondestructive Testing and Chairman of Subcommittee E07.07 on Electromagnetic Methods. He is also a member of IEEE, ASNT, and the honor societies Sigma Xi, Tau Beta Pi and Eta Kappa Nu. He is an expert in physics-based modeling and has contributed to numerous patens and papers. His experience includes writing data acquisition and analysis software and the use of several commercial analysis packages and finite element packages. Andy is also part of the team that won the FAA/Air Transport Association 2007 "Better Way" Award for engine component inspection technology.

24

Patents issued and pending

Dr. Darrell Schlicker, Director of Instrumentation.

Dr. Schlicker specializes in the development of sensors and optimal instrumentation to realize full sensing capability. His areas of expertise include modeling of electromagnetic systems, analog filter design, analog and digital system design, development of tools for automating the design process, multi-processor instrumentation and optimal intra-communication protocols, and the development of modular, scalable, multi-sensor architectures. His software/ firmware development experience includes object-oriented approaches to multi-device systems, numerical algorithms for solving electromagnetic systems, embedded firmware in instruments, embedded firmware for multi-processor systems, and GUIs under Windows. His mechanical design experience includes low-parasitic electrical housing and interconnects for sensors, specialized instrumentation packaging, and sensor calibration/actuation systems. Dr. Schlicker has his Ph.D. and M.S. degrees from MIT where he completed his thesis work in the Laboratory for Electromagnetic and Electronic Systems, and a Bachelor's Degree in Electrical Engineering from Michigan Technological University. Since joining JENTEK, Dr. Schlicker has contributed to numerous patents and papers. He is also part of the JENTEK team that won the FAA/Air Transport Association 2007 "Better Way" Award for engine component inspection technology.

Dr. Neil J. Goldfine, Founder and President.

Dr. Goldfine founded JENTEK Sensors in January 1992. He is a specialist in sensor design, measurement optimization and continuum modeling for nondestructive evaluation, materials characterization and control of electromagnetic and electromechanical systems and processes. He is also a Research Affiliate at the M.I.T. Laboratory for Electromagnetic and Electronic Systems, where he participates in research in sensor design, system identification, and electromagnetic modeling of sensors. He was an Associate Technical Editor of the ASNT Materials Evaluation Magazine from October 1996 to July 2005. Prior to starting JENTEK Sensors, Dr. Goldfine worked as a Financial and Market Analyst at H & Q Technology Partners (a management consulting and investment banking firm founded by former Secretary of Defense, William Perry). Dr. Goldfine is widely published in the NDE field, particularly in the area of aging aircraft applications. Dr. Goldfine has contributed to over 30 patents. He has been principal investigator on several SBIR Phase II programs and larger government contracts for NASA, Air Force, Navy, DOE, DOT, Army and FAA. He has managed JENTEK's R&D programs since the company was founded in 1992. His academic honors and awards include: Ford Motor Co. Fellowship, 1984; Hugo Otto Wolf Memorial Award for Originality of Work in Electrical Engineering, 1982; and Kodak Prize for Academic Excellence in Electrical Engineering, 1981. He has been a member of the engineering honor societies Tau Beta Pi and Eta Kappa Nu. Dr. Goldfine has both a Master's Degree and Ph.D. in Mechanical Engineering from M.I.T., as well as Bachelor's Degrees in Mechanical and Electrical Engineering from the University of Pennsylvania. He also completed the majority of course work in Management as a Masters student at MIT Sloan School before leaving MIT in 1990.

Dr. Goldfine has also led JENTEK Sensors to receive several awards and honors, including the following: (1) FAA/Air Transport Association 2007 "Better Way" Award for engine component inspection technology, (2) 2006 National Tibbetts Award, (3) Outstanding Phase III Transition Award, 2004, awarded by the Navy Transition Assistance Program, and (4) Outstanding Paper Award, titled: "Eddy Current Sensor Networks for Aircraft Fatigue Monitoring," published in ASNT *Materials Evaluation* Magazine, July 2003, Vol.61, No.7. He has also contributed to chapters and other sections to prestigious publications, including:

25

Patents issued and pending

Goldfine, N., Washabaugh, A., Sheiretov, Y., Windoloski, M. (2009). Eddy-current Methods, in *Encyclopedia of Structural Health Monitoring*, Boller, C., Chang, F. and Fujino, Y. (eds). John Wiley & Sons Ltd, Chichester, UK, pp 393-412.

Goldfine, N., Zilberstein, V., Schlicker, D., Grundy, D. (2009) Eddy-current in situ Sensors for SHM, in *Encyclopedia of Structural Health Monitoring*, Boller, C., Chang, F. and Fujino, Y. (eds). John Wiley & Sons Ltd, Chichester, UK, pp 1051-1064.

Goldfine, N. (1999). "Commercialization: from Basic Research to Sales to Profits," *Ultrasonic Instruments and Devices II, Physical Acoustics XXIV*, Thurston, R., Pierce, A., Papadakis, E. (eds), Academic Press, pp 15-19.

Patents issued and pending